PHYSICAL REVIEW D VOLUME 13, NUMBER 4 15 FEBRUARY 1976

Strong-coupling calculations of lattice gauge theories: (1 + 1)-dimensional exercises

T. Banks and Leonard Susskind*
Tel Aviv University, Tel Aviv, Israel

John Kogut†
Laboratory of Nuclear Studies, Cornell University, Ithaca, New York 14853
(Received 25 August 1975)

Strong-coupling methods for solving gauge theories formulated on a lattice are illustrated by studying the lattice version of the massive Schwinger model. The vacuum state of the model spontaneously breaks chiral symmetry and is equivalent to an Ising antiferromagnetic chain. Several lattice perturbation-theory calculations are carried out to fourth order in the dimensionless expansion parameter $1/g^2a^2$, where a is the lattice spacing. Padé approximants are then employed to extrapolate the calculations to large $1/g^2a^2$. Good agreement between these calculations and exact results on the continuum massive Schwinger model are found.

I. INTRODUCTION

It is hoped that lattice gauge theories will make possible practical calculations in the field of strong interactions. In addition, the theory is believed to be as fundamental as any presently conceived. The dictate of local color gauge invariance is the central idea of the theory and it greatly restricts the form of the theory's Hamiltonian and physical subspace. The reason for introducing the lattice is simple: It allows numerical analysis of the theory even if it is strongly coupled. These methods bear a strong resemblance to the high-temperature expansion used in statistical mechanics to solve spin lattice models of magnetism. Although the lattice destroys the usual space-time symmetries (so dear to particle physicists), it allows color gauge invariance (so dear to the authors) to be formulated precisely. If the strong-coupling calculational methods are successful, then the lattice will not appear in the real solution of the theory—the lattice will have played the role of scaffolding and the space-time symmetries of relativistic quantum field theory will be retrieved when the hard work is completed. The formulation of lattice theories and pedagogical discussions of their fundamentals can be found in Refs. 1–4.

It is the purpose of this article to illustrate Hamiltonian lattice gauge theory[2] calculations for some simple models. Our motivation in undertaking these exercises is to determine a simple calculational scheme for composite-particle masses and to work out enough orders of strong-coupling perturbation theory to allow a comparison of these results to answers obtained by more conventional means. To that end we considered the simplest lattice gauge theories of all—the massive and massless Schwinger models.[5,6] After considerable bumbling about with sophisticated methods we found that plain old Rayleigh-Schrödinger perturbation theory, improved via Padé approximants, is a simple and surprisingly accurate calculational scheme. Several strong-coupling calculations carried to fourth order in $1/g^2a^2$ and improved via Padé approximants are in good agreement with the corresponding calculations in the continuum theories. The calculations themselves are very easy (there are no complicated integrals or sums in lattice perturbation theory), and this success makes us optimistic about applying these methods to (3+1)-dimensional, non-Abelian gauge theories. Although it may be necessary to carry lattice perturbation theory to a very high order to see the continuum limit appear, approximate but meaningful calculations of the theory's mass spectrum may be accomplished by less Herculean efforts.

This article is organized into five sections. First, we formulate the massive Schwinger model on a spatial lattice. Some care is needed in placing fermions on a lattice such that the Dirac equation occurs in the continuum limit. This is accomplished using the staggered lattice described in Ref. 2. Finally, the Fermi fields are eliminated in favor of spin matrices using the Jordan-Wigner transformation.[7] In Sec. III the first element of strong-coupling perturbation theory is described. This is the determination of the vacuum state of the theory. By a second-order perturbation theory calculation we find that the vacuum is the ground state of an Ising antiferromagnetic chain. This is a state which breaks chiral invariance by having $\langle\bar{\psi}\psi\rangle_0 \neq 0$. The calculation of the mass of the vector boson in the (massive) Schwinger model appears in Sec. IV. Strong-coupling perturbation theory is carried out through fourth order, and the expansion is interpreted as a diagonal Padé approximant. For a large range of the expansion parameter $1/g^2a^2$ the energy of the state lies near the value it has in the continuum theory. Similar

calculations of the mass of a scalar state are also carried out. These calculations support a plausible argument that there is a stable two-boson bound state in the massive Schwinger model. These results are discussed and some remarks on related calculations which are in progress are made in the concluding section.

II. FERMIONS ON A LATTICE

The continuum formulations of the original Schwinger model[5] (QED with massless fermions in 1+1 dimensions) and the massive Schwinger model[6] have been widely discussed recently. The massive model is a well-behaved, interacting theory of quark confinement in which gauge invariance is an exact symmetry of the states.[6] It is a good laboratory for the (3+1)-dimensional problem of interest. Our first task in studying its lattice version is to formulate the fermion field on a spatial lattice. We follow Ref. 2 here and employ a staggered lattice. We use this method for two reasons: It is convenient and it works. (The reader can convince himself that seemingly simpler lattice constructions, e.g. putting two-component fields on each lattice site, do not give the Dirac equation in the continuum limit.) Consider a spatial lattice (continuous time) with a lattice spacing a. Label the lattice sites with an integer n. There will be a one-component fermion field $\phi(n)$ at each site n. $\phi(n)$ satisfies the anticommutation relation

$$\{\phi^\dagger(n), \phi(m)\} = \delta_{n,m}, \quad \{\phi(n), \phi(m)\} = 0. \tag{2.1}$$

$\phi(n)$ is related to a properly normalized continuum field χ having canonical anticommutation relations by

$$\phi(n) = \sqrt{a}\,\chi(x). \tag{2.2}$$

Consider the Hamiltonian

$$H = \frac{i}{2a}\sum_n [\phi^\dagger(n)\phi(n+1) - \phi^\dagger(n+1)\phi(n)]. \tag{2.3}$$

We claim that with a proper identification of a two-component fermion field Eqs. (2.1)–(2.3) generate the massless Dirac equation in the continuum limit. First compute

$$i[H, \phi(n)] = \dot{\phi}(n) = \frac{\phi(n+1) - \phi(n-1)}{2a}. \tag{2.4}$$

Note that the time dependence of $\phi(n)$ at even (odd) sites is determined by the spatial difference of $\phi(n\pm 1)$ at odd (even) sites. So, to ensure finite time dependence in $\phi(n)$ at even (odd) sites, we must require that the spatial dependence in $\phi(n)$ at odd (even) sites be smooth. Thus we define a two-component field $\psi(n)$ as follows:

$$\psi = \begin{pmatrix} \psi_e \\ \psi_o \end{pmatrix}, \qquad \psi_e(n) = \phi(n), \quad n \text{ even}, \qquad \psi_o(n) = \phi(n), \quad n \text{ odd}. \tag{2.5}$$

Then the components of $\psi(n)$ satisfy the equations

$$\dot{\psi}_o = \frac{\Delta\psi_e}{\Delta x}, \quad \dot{\psi}_e = \frac{\Delta\psi_o}{\Delta x}, \tag{2.6}$$

where Δ indicates the discrete difference in Eq. (2.4). Note that Eq. (2.6) becomes the massless Dirac equation in the continuum limit,

$$\frac{\partial}{\partial t}\psi = \begin{pmatrix} 0 & 1 \\ 1 & 0 \end{pmatrix}\frac{\partial}{\partial x}\psi \tag{2.7}$$

in a standard basis where

$$\gamma_0 = \begin{pmatrix} 1 & 0 \\ 0 & -1 \end{pmatrix}.$$

One-dimensional fermion problems can be written in terms of one-dimensional spin problems by using a transformation invented long ago by Jordan and Wigner.[7] Let $\sigma_i(n)$ denote a spin matrix at each site. Define also $\sigma^\pm(n) = [\sigma_1(n) \pm i\sigma_2(n)]/2$. Then a representation for the fermion field $\phi(n)$ is

$$\phi(n) = \prod_{l<n}[i\sigma_3(l)]\sigma^-(n), \qquad \phi^\dagger(n) = \prod_{l<n}[-i\sigma_3(l)]\sigma^+(n). \tag{2.8}$$

One easily confirms that these relations reproduce the fundamental anticommutation relations of the fermion field stated in Eq. (2.1). The Hamiltonian, Eq. (2.3), is simple in terms of the spin operators. Since

$$\phi^\dagger(n)\phi(n+1) = -i\sigma^+(n)\sigma^-(n+1),$$

we have

$$H = \frac{1}{2a}\sum_n [\sigma^+(n)\sigma^-(n+1) + \sigma^+(n+1)\sigma^-(n)]. \tag{2.9}$$

Therefore, as is well known, the free massless Dirac field on a spatial lattice is equivalent to an XY antiferromagnetic chain of spins.[8]

Next we note the form of the Dirac bilinears when written in terms of spin matrices. First the charge density becomes

$$j^0=\tfrac{1}{2}[\psi^\dagger,\psi]=\tfrac{1}{2}[\psi_e^\dagger,\psi_e]+\tfrac{1}{2}[\psi_o^\dagger,\psi_o]\longrightarrow\tfrac{1}{2}[\phi^\dagger(n),\phi(n)]=\tfrac{1}{2}[\sigma^+(n),\sigma^-(n)]=\tfrac{1}{2}\sigma_3(n), \tag{2.10a}$$

the scalar density becomes

$$\bar{\psi}\psi=\psi_e^\dagger\psi_e-\psi_o^\dagger\psi_o\longrightarrow(-1)^n\phi^\dagger(n)\phi(n)=(-1)^n\tfrac{1}{2}[1+\sigma_3(n)], \tag{2.10b}$$

the axial-vector density, which is also the vector flux, becomes

$$j_5^0=\psi^\dagger\gamma_5\psi=\psi_e^\dagger\psi_o+\psi_o^\dagger\psi_e\longrightarrow\phi^\dagger(n)\phi(n+1)+\phi^\dagger(n+1)\phi(n)=-i[\sigma^+(n)\sigma^-(n+1)-\sigma^+(n+1)\sigma^-(n)], \tag{2.10c}$$

and the pseudoscalar density becomes

$$i\bar{\psi}\gamma_5\psi=i(\psi_o^\dagger\psi_e-\psi_e^\dagger\psi_o)\longrightarrow+i[\phi^\dagger(n+1)\phi(n)-\phi^\dagger(n)\phi(n+1)]=[\sigma^+(n+1)\sigma^-(n)+\sigma^+(n)\sigma^-(n+1)]. \tag{2.10d}$$

It is interesting that the axial charge $Q_5=\int j_5^0(x)dx$ interchanges ψ_e with ψ_o. Therefore, it can be interpreted as a translation of the lattice by one unit in a. The momentum operator, on the other hand, has the continuum form, $p_1=\int\psi(-i\partial_1)\psi dx$. Since the discrete form of the gradient ∂_1 connects only even or odd sites [cf. Eq. (2.4)], the discrete form of p_1 translates the lattice by $2a$.

III. MASSIVE SCHWINGER MODEL ON A LATTICE

The formulation of gauge theories on a spatial lattice has been discussed and reviewed elsewhere in considerable detail.[1-4] We assume that the reader is familiar with these ideas and turn directly to a specialization to Abelian models in 1+1 dimensions. Recall that fermion fields are defined on sites as described above and that the gauge field,

$$U(n,n+1)=e^{iagA(n)}\equiv e^{i\theta(n)}, \tag{3.1}$$

is defined on links. The quantity $A(n)$ is the spatial component of the Abelian vector potential. We always work in the class of gauges with $A^0=0$ in order to have a simple Hamiltonian and space of states.[2] In this gauge the electric field, which is canonically conjugate to A, is $\dot{A}$. The discrete form of the canonical commutation relations of the gauge field is

$$[A(n),E(m)]=i\frac{1}{a}\delta_{n,m}. \tag{3.2}$$

Since the vector potential A will only enter the lattice theory through the operator $e^{i\theta}=e^{iagA}$, the physically meaningful range of A is

$$0\le\theta(n)<2\pi,\quad 0\le agA(n)<2\pi. \tag{3.3}$$

Define the operator $L(n)$ which generates cyclic translations in the variable $\theta(n)$,

$$[\theta(n),L(m)]=i\delta_{n,m}. \tag{3.4}$$

It follows from Eq. (3.1) and (3.2) that $L(m)$, an angular momentum operator, is

$$L(m)=\frac{1}{g}E(m). \tag{3.5}$$

Because of Eqs. (3.3) and (3.4) the possible values of $L(m)$ are quantized in steps of $0,\pm1,\pm2,\ldots$. This quantization of electric flux also occurs in the continuum Schwinger model—it follows from Gauss's law and the lack of transverse dimensions of space.

The operators $L(m)$ and $\exp[i\theta(m)]$ can be represented simply on a ladder space $\{|l\rangle\}$ consisting of eigenstates of $L(m)$,

$$L|l\rangle=l|l\rangle,\quad l=0,\pm1,\pm2,\ldots. \tag{3.6}$$

It follows from Eq. (3.4) that $\exp[\pm i\theta(m)]$ are the raising and lowering operators,

$$e^{\pm i\theta}|l\rangle=|l\pm1\rangle. \tag{3.7}$$

Now we pass to the Hamiltonian. The gauge-field piece is the discrete form of $\frac{1}{2}\int E(x)^2dx$,

$$H_G=\tfrac{1}{2}\sum_n E^2(n)a=\tfrac{1}{2}g^2a\sum_n L^2(n). \tag{3.8}$$

Since $L(n)$ takes on the values $0,\pm1,\pm2,\ldots$, the last form of H_G is particularly illuminating. Next we must couple the gauge field to the fermions. The requirement of local gauge invariance specifies how this is done. Recall that a point-separated operator, such as $\bar{\psi}(x+\epsilon)\gamma^\mu\gamma_5\psi(x)$, is gauge invariant for arbitrary ϵ only if it is multiplied by the phase[9]

$$\exp\left(ie\int_x^{x+\epsilon}A_\mu(x)dx^\mu\right).$$

Therefore, to render the kinetic-energy portion of the fermion Hamiltonian Eq. (2.9) gauge invariant we modify it to

$$H_f=\frac{1}{2a}\sum_n[\sigma^+(n)e^{i\theta(n)}\sigma^-(n+1)+\text{H.c.}]. \tag{3.9}$$

As discussed in Ref. 2 the sum $H_G + H_f$ reproduces the familiar massless Schwinger model in the continuum $a \to 0$ weakly coupled limit. In summary, the lattice Hamiltonian is

$$H = \tfrac{1}{2} g^2 a \sum_n L^2(n) + \frac{1}{2a} \sum_n [\sigma^+(n) e^{i\theta(n)} \sigma^-(n+1) + \text{H.c.}]. \tag{3.10}$$

Now we wish to solve for the eigenstates of H. If one considers the dimensionless parameter $g^2 a^2$ to be large (strong coupling), then one can apply standard perturbation theory methods here. Write

$$W = \frac{2}{a g^2} H = H_0 + H_{\text{int}} = H_0 + xV, \tag{3.11}$$

where

$$H_0 = \sum_n L^2(n), \qquad V = \sum_n [\sigma^+(n) e^{i\theta(n)} \sigma^-(n+1) + \text{H.c.}] \tag{3.12a}$$

and

$$x = \frac{1}{g^2 a^2}. \tag{3.12b}$$

For $x \ll 1$ one can treat H_{int} as a perturbation on H_0. The first problem one faces here is the enormous degeneracy of the unperturbed Hamiltonian H_0: This operator contains no reference to the fermion fields, so states which are fluxless but have any configuration of $\phi(n)$ are degenerate. Therefore, we must apply degenerate perturbation theory and first diagonalize the perturbation in the degenerate subspace. The first nonzero perturbation occurs in order x^2 and reads

$$\delta E = x^2 \left\langle \phi, L = 0 \left| V \frac{1}{-H_0} V \right| \phi, L = 0 \right\rangle, \tag{3.13}$$

where the notation $\langle \phi, L = 0|$ indicates a fluxless [$L^2(n) = 0$ for all n] state with a fermion configuration ϕ which will be determined by minimizing δE. We compute

$$\begin{aligned} \delta E &= -x^2 \left\langle \phi, L = 0 \left| \sum_{n,m} [\sigma^+(n) e^{i\theta(n)} \sigma^-(n+1) + \text{H.c.}][\sigma^+(m) e^{i\theta(m)} \sigma^-(m+1) + \text{H.c.}] \right| \phi, L = 0 \right\rangle \\ &= -x^2 \left\langle \phi, L = 0 \left| \sum_n [\sigma^+(n)\sigma^-(n+1)\sigma^+(n+1)\sigma^-(n) + \text{H.c.}] \right| \phi, L = 0 \right\rangle \\ &= -\tfrac{1}{2} x^2 \left\langle \phi, L = 0 \left| \sum_n [1 + \sigma_3(n)][1 - \sigma_3(n+1)] \right| \phi, L = 0 \right\rangle. \end{aligned} \tag{3.14}$$

Since $\frac{1}{2}[1 \pm \sigma_3(n)]$ is either 0 or 1, the minimization of δE is the same problem as finding the ground state of an Ising antiferromagnetic chain. To minimize Eq. (3.14) one wants $\frac{1}{4}[1 + \sigma_3(n)][1 - \sigma_3(n+1)]$ to be +1 on as many sites as possible. There are two ways to do this: $\sigma_3(n) = +1$ (-1) on all even (odd) sites or vice versa.

Finally we should generalize these considerations to the massive Schwinger model. It follows from the correspondences in Eq. (2.10) that H_0 becomes

$$H_0 = \sum_n L^2(n) + \tfrac{1}{2} \mu \sum_n (-1)^n \sigma_3(n), \tag{3.15}$$

where

$$\mu = 2m/g^2 a$$

and V remains unchanged. The mass now introduces explicit symmetry breaking into the Hamiltonian and it determines which of the two antiferromagnetic vacuums discussed for the massless model is the vacuum. Clearly the state with $\sigma_3(n) = +1$ for odd sites and -1 for even sites is the lower-energy state. We define this state as zero energy in the perturbation-theory calculations which follow.

IV. STRONG-COUPLING CALCULATIONS

Our task here is to calculate the mass of the boson in the massive Schwinger model to order x^4 in Rayleigh-Schrödinger perturbation theory suitably improved by Padé approximants. In the continuum theory this state is generated by applying the vector flux $j' = j_5^0$ to the vacuum. To be properly defined the flux must be point-separated and manifestly gauge invariant. The most local lattice construction of this state with zero momentum is therefore

$$|1-\rangle = \sum_m [\sigma^+(n) e^{i\theta(n)} \sigma^-(n+1) - \text{H.c.}] |0\rangle .$$

FIG. 1. Action of V on the vacuum.

Its unperturbed energy is

$$\epsilon_1 = 1 + 2\mu. \tag{4.1}$$

The first term of Eq. (4.1) records the energy of the flux line and the 2μ gives the energy of the $q\bar{q}$ relative to the vacuum. The factor of 2 comes about as follows. When the factor $\sigma^+(n)e^{i\theta(n)}\sigma^-(n+1)$ + H.c. is applied to the vacuum it raises (lowers) $\sigma_3(n)$ at even (odd) sites. Thus the change in energy at the even site is $\frac{1}{2}\mu$ [the final value of $\frac{1}{2}\mu\sigma_3(n)$] minus $-\frac{1}{2}\mu$ [the initial value of $\frac{1}{2}\mu\sigma_3(n)$ in the vacuum]. Next consider the effects which can be caused by V in Eq. (3.10a). When V acts on the vacuum, it flips the spins at adjacent sites and puts a flux line between them as depicted in Fig. 1. The numerical value of the vertex is unity and its action on the vacuum will be represented diagrammatically as in Fig. 2. Note that there is a relative minus sign between the vertices in Figs. 2(a) and 2(b) because of the relative minus sign in Eq. (2.3). Now apply V to a state in which there is a single boson as shown in Fig. 1. An alternative simplified figure depicting the boson is shown in Fig. 3. If a term in V overlaps completely with the vector meson it can be destroyed. We shall represent this possibility by Fig. 4(a), which is related by Hermiticity to Fig. 4(b). Note that no term in V can act at a site adjacent to the vector meson— since the spins adjacent to the boson in Fig. 1 are either both up or both down, a term in V which lies on these links gives zero. However, V can act on any other link and create virtual mesons.

To carry time-independent perturbation theory to high order requires considerable care. Let E denote the exact energy of an eigenstate of H. Then E can be calculated by Wigner-Brillouin perturbation theory[10]:

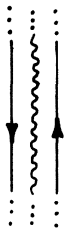

FIG. 3. A vector-meson state. The $q\bar{q}$ are separated by one link and one unit of flux.

$$E = \epsilon + xV + x^2V\frac{1-P}{E-H_0}V + x^3V\frac{1-P}{E-H_0}V\frac{1-P}{E-H_0}V + \cdots, \tag{4.2}$$

where ϵ is the unperturbed energy of the state and P is a projection operator onto the initial state. Equation (4.2) has the advantage of proceeding to arbitrarily high orders in V in a simple way. However, it is an implicit equation for the desired energy E. The more familiar Rayleigh-Schrödinger perturbation theory is obtained by writing E in the form of an expansion,

$$E = \epsilon + \sum_{n=1}^{\infty} c_n x^n, \tag{4.3}$$

substituting into Eq. (4.2), and matching coefficients to the desired accuracy. As will be explained below, only even powers of V contribute to Eq. (4.2) for our lattice theory, so we write

$$E = \epsilon + ax^2 + bx^4 + \cdots \tag{4.4}$$

and solve for a and b,

$$\begin{aligned} a &= V\frac{1-P}{\epsilon - H_0}V, \\ b &= V\frac{1-P}{\epsilon-H_0}V\frac{1-P}{\epsilon-H_0}V\frac{1-P}{\epsilon-H_0}V \\ &\quad -\left(V\frac{1-P}{\epsilon-H_0}V\right)\left(V\frac{1-P}{(\epsilon-H_0)^2}V\right). \end{aligned} \tag{4.5}$$

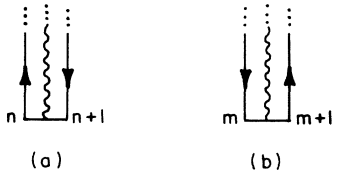

FIG. 2. (a) The vertex V acting on an even site (n = even)—odd site. (b) The vertex V acting on an odd site—even site.

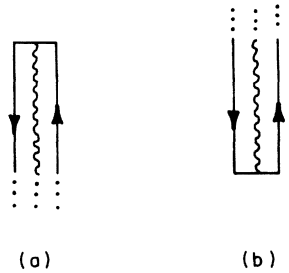

FIG. 4. (a) V destroys a vector meson. (b) V creates a vector meson.

FIG. 5. Second-order contribution to the vacuum energy, E_0.

The terms through $O(x^2)$ are simple and familiar, but the term of $O(x^4)$ has a correction due to the mismatch at $O(x^2)$ between ϵ and E. In the calculations to follow, we evaluate these equations for the single-particle state and obtain E_1 through fourth order. The perturbation also shifts the energy of the vacuum, so we must calculate its energy E_0 through fourth order and identify the difference $E_1 - E_0$ as the meaningful calculation of the mass of the meson.

It is convenient to have a diagrammatic interpretation of Eqs. (4.4) and (4.5) which uses the conventions stated in Figs. 2–4. Vertices and states are indicated as in those figures. Terms in the perturbation expansion are diagrammed by figures which proceed from the bottom of the figure (initial state) to the top of the figure (final state). Intermediate states and their corresponding energy denominators are indicated by horizontal slices bounded above and below by vertices.

Consider the second-order calculation of $E_1 - E_0$ in detail. The graphs which contribute are shown in Figs. 5–9. First consider the shift of the vacuum energy, Fig. 5. Clearly this contribution is proportional to the number of links in the lattice. Since our desired quantity (the mass of the meson) is intensive, this vacuum shift must cancel against Fig. 6. To see the cancellation and retrieve the finite remainder, we compute all quantities on a lattice of N links (periodic boundary conditions), and explicitly verify the required cancellations. This method, although rather pedestrian, is very reliable. The vacuum graph in

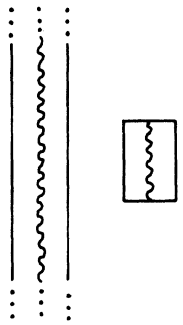

FIG. 6. Second-order disconnected graph contributing to E_1.

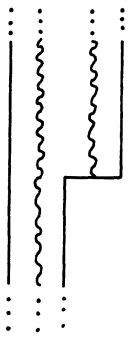

FIG. 7. A forbidden graph.

Fig. 5 contributes to E_0

$$N\left(\frac{x^2}{-1-2\mu}\right) \tag{4.6}$$

since there are N links, a factor of x for each vertex, and an energy denominator, $\epsilon_0 - H_0 = 0 - (1+2\mu)$. The disconnected graph in Fig. 6 contributes to E_1

$$(N-3)\frac{x^2}{\epsilon_1 - 2(1+2\mu)} = (N-3)\left(\frac{x^2}{-1-2\mu}\right). \tag{4.7}$$

The counting factor $(N-3)$ records the number of links on which the vacuum fluctuation can occur—it cannot occur on any link which has at least one site in common with the throughgoing particle state. The reason for this rule, which stems from the form of the vacuum, was explained in the first paragraph of this section. In particular, it prohibits any graph of the form shown in Fig. 7 and guarantees that only the even terms in Eq. (4.2) occur for this theory. Thus, the theory's expansion parameter is really $y = x^2$. We shall use the variable y everywhere below. The final contributing graphs involve no vacuum structure and are illustrated in Figs. 8(a) and 8(b). Figure

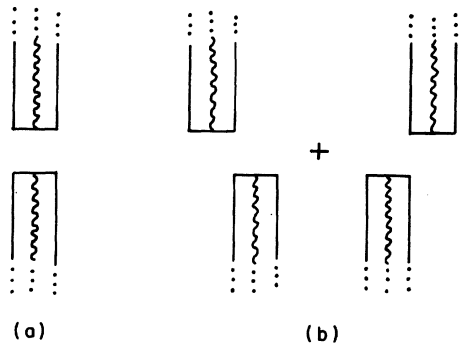

FIG. 8. Graphs without vacuum structure which contribute to E_1 in second order.

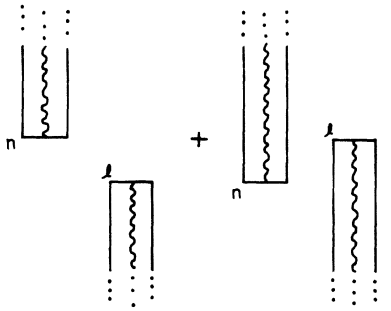

FIG. 9. Two graphs whose sum vanishes. The integers n and l label sites.

8(a) gives

$$\frac{y}{1+2\mu} \tag{4.8a}$$

and Fig. 8(b) gives

$$2(-1)\left(\frac{y}{1+2\mu}\right). \tag{4.8b}$$

The minus sign in Eq. (4.8b) is the same minus sign which exists between the two graphs shown in Figs. 2(a) and 2(b). Graphs having the same form as those in Fig. 8(b), but in which at least one link appears between the initial and final meson, cancel in pairs. This is shown in Fig. 9; the two time orderings are equal in magnitude and opposite in sign.

Let us collect the results obtained so far:

$$E_1 - E_0 = 1 + 2\mu + \frac{2y}{1+2\mu}. \tag{4.9}$$

Now we shall sketch the calculation of the fourth-order contributions to $E_1 - E_0$. There are four

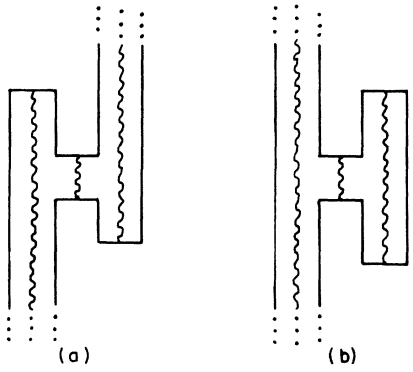

FIG. 10. Connected fourth-order contributions to E_1.

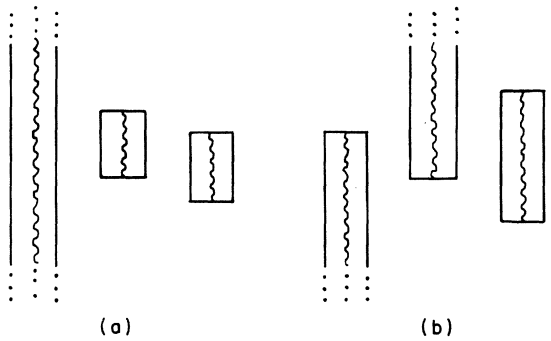

FIG. 11. Disconnected contributions to E_1. Other time orderings of these basic graphs must also be computed.

types of contributions: connected particle graphs (Figs. 10), disconnected graphs (Figs. 11), vacuum graphs (Fig. 12), and the calculation of the second term in b, Eq. (4.5), for the single-particle and vacuum states. The connected particle graphs contribute as follows:

$$\text{Fig. 10(a)}: \frac{2}{(-2)(1+2\mu)^2} \tag{4.10a}$$

$$\text{Fig. 10(b)}: \frac{2}{(-2)(1+2\mu)^2}\,. \tag{4.10b}$$

The disconnected graphs give the following contributions.

$$\text{Fig. 11(a)}: \frac{4}{(-2)(1+2\mu)^3}\frac{(N-5)(N-4)}{2} \tag{4.11a}$$

$$\text{Fig. 11(b)}: \frac{4}{(-2)(1+2\mu)^3}(N-4). \tag{4.11b}$$

The calculation of the counting factors requires some care. For Fig. 11(a), given the position of the particle state, the boxes can be placed anywhere such that no lines overlap. Therefore, the first box can occupy $(N-3)$ sites and the second box $(N-6)$ sites, neglecting the possibility that the first box is separated by only one link from the throughgoing particle. In the two cases where the first box and the particle are separated by one link, there are $(N-5)$ positions available to the second box. Thus there are $(N-3)(N-6)+2$

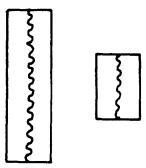

FIG. 12. Fourth-order contribution to E_0.

$= (N-4)(N-5)$ ways of making this contribution. Finally this result must be divided by 2 because the two boxes are identical. The factor of 4 records the number of different orderings of the four vertices (different time orderings), each of which contributes an energy denominator $[-2(1+2\mu)^3]^{-1}$. Next consider the expression for Fig. 11(b). The factor of 4 comes from the four time orderings shown in Fig. 13. Each graph contributes the same energy denominator as for Fig. 11(a). Finally, in determining the counting factor care must be used since graphs with an odd (even) number of links separating the initial and final particles carry the sign + 1 (− 1). Continuing, the vacuum graphs of Fig. 12 contribute

$$\frac{4}{(-2)(1+2\mu)^3}\frac{N(N-3)}{2}. \tag{4.12}$$

Finally one must calculate the quantities of Eq. (4.5),

$$\left(V\frac{1-P}{\epsilon-H_0}V\right)\left(V\frac{1-P}{(\epsilon-H_0)^2}V\right), \tag{4.13}$$

for the vacuum and the single-particle state. These evaluations are as easy as the second-order ones. However, since the square of an energy denominator appears in Eq. (4.13), one must be careful with signs. For the vacuum we find

$$\left\langle 0\left|V\frac{1-P_0}{-H_0}V\right|0\right\rangle\left\langle 0\left|V\frac{1-P_0}{H_0^2}V\right|0\right\rangle=\frac{N^2}{(1+2\mu)^3}, \tag{4.14}$$

and for the single-particle state

$$\left\langle 1\left|V\frac{1-P_1}{\epsilon_1-H_0}V\right|1\right\rangle\left\langle 1\left|V\frac{1-P_1}{(\epsilon_1-H_0)^2}V\right|1\right\rangle = \frac{(N-2)^2}{(1+2\mu)^3}. \tag{4.15}$$

Finally, we collect these results and record E_1-E_0:

$$E_1-E_0=1+2\mu+\left(\frac{2}{1+2\mu}\right)y+\left(\frac{-4\mu-10}{(1+2\mu)^3}\right)y^2+\cdots. \tag{4.16}$$

According to Eq. (3.9), this quantity is

$$E_1-E_0=\frac{2}{ag^2}m_-=2y^{1/4}\frac{m_-}{g}, \tag{4.17}$$

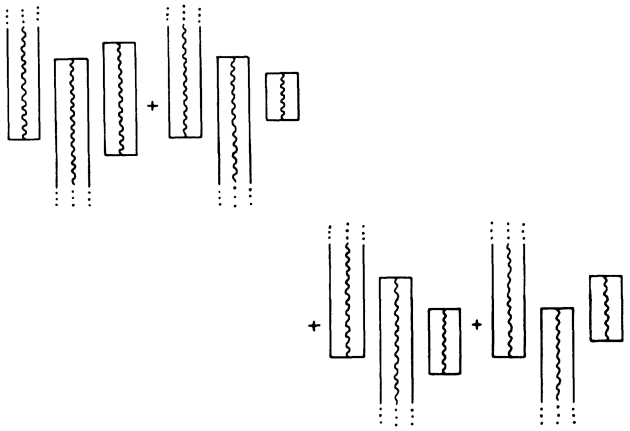

FIG. 13. The four nonzero time orderings of Fig. 11(b).

where m_- is the mass of the boson.

Equation (4.16) gives us the behavior of the mass m_- for small values of $y = 1/a^4g^4$, i.e., large values of g^4a^4. To compare with continuum field theory results, we are in fact interested in the limit $g^4a^4 \to 0$. To make the extrapolation from small y to large y, we follow our statistical-mechanics colleagues and form the [1, 1] Padé approximant[11] of the power series in Eq. (4.16):

$$2y^{1/4}\frac{m_-}{g}=(1+2\mu)\frac{(1+2\mu)^2+(7-2\mu)y}{(1+2\mu)^2+(5-2\mu)y}. \tag{4.18}$$

Since

$$\mu=\frac{2m}{g^2a}=\frac{2m}{g}y^{1/4}, \tag{4.19}$$

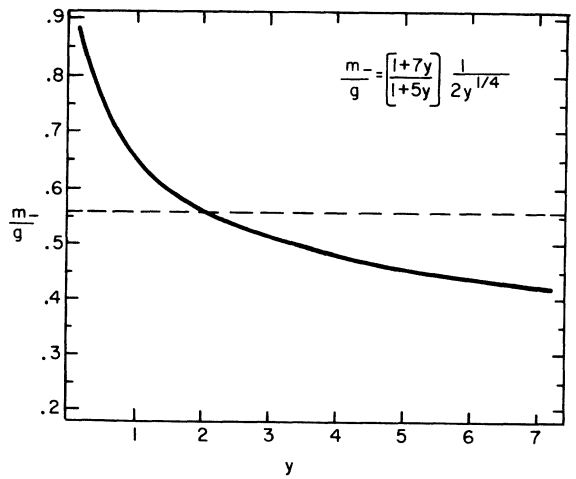

FIG. 14. A plot of Eq. (4.21). The desired result is the dashed horizontal line.

we have finally

$$\frac{m_-}{g}=\left(\frac{1}{2y^{1/4}}+\frac{2m}{g}\right)\times\frac{[1+(4m/g)y^{1/4}]^2+[7+(4m/g)y^{1/4}]y}{[1+(4m/g)y^{1/4}]^2+[5+(4m/g)y^{1/4}]y}. \quad (4.20)$$

Let us compare this result with the massless Schwinger model[5] in which $m_-/g=1/\sqrt{\pi}=0.564$. For $m=0$, Eq. (4.20) simplifies to

$$\frac{m_-}{g}=\left(\frac{1+7y}{1+5y}\right)\frac{1}{2y^{1/4}}, \quad (4.21)$$

which is plotted in Fig. 14. We observe that for a wide range of y the curve remains close to the continuum result 0.564. Unfortunately, Eq. (4.21) cannot be extrapolated sensibly to $y\to\infty$ using just the [1, 1] Padé approximant. There are two ways to cure this fault. First, higher-order calculations of m_-/g will allow the construction of the [2, 2], [3, 3], etc. Padé approximants. If the lattice theory is behaving properly then the higher-order analogs of Eq. (4.21) will closely approximate $1/\sqrt{\pi}$ for larger ranges of y. No single diagonal Padé approximant can be extrapolated to $y\to\infty$, but the trend for the $[m,m]$ Padé expressions to closely approximate $1/\sqrt{\pi}$ for larger and larger y should become clear. A second way to cure the fault is to extrapolate the power series Eq. (4.10) by using the form

$$\frac{(1+by)^{5/4}}{1+ay}. \quad (4.22)$$

Then,

$$\frac{m_-}{g}=\frac{1}{2y^{1/4}}\frac{(1+by)^{5/4}}{1+ay}\xrightarrow[y\to\infty]{}\frac{1}{2}\frac{b^{5/4}}{a}. \quad (4.23)$$

In the present case this method gives

$$\frac{m_-}{g}\cong 0.814, \quad (4.24)$$

which is 30% above the continuum value. It would be interesting to see if this extrapolation procedure improves in higher orders.

Next we shall calculate the mass of the scalar state

$$|1+\rangle=\sum_n[\sigma^+(n)e^{i\theta(n)}\sigma^-(n+1)+\text{H.c.}]|0\rangle.$$

The identification of this object with a scalar at zero momentum follows from Eq. (2.10d). The calculation proceeds just as for the $|1-\rangle$ state except that the weight (-1) for graphs with an odd number of links separating initial and final scalar particles is absent. The topologies of the second- and fourth-order graphs are the same as those in Figs. 5–13. The counting factors must be recalculated for Fig. 8 and Fig. 11(b) because of the different sign considerations. The result of this exercise is

$$W=2\sqrt{x}\,\frac{m_+}{g}=1+2\mu+\left(\frac{6}{1+2\mu}\right)x^2-\left(\frac{4\mu+26}{(1+2\mu)^3}\right)x^4. \quad (4.25)$$

The [1, 1] Padé approximant for Eq. (4.25) reads

$$\frac{m_+}{g}=\left(\frac{1}{2y^{1/4}}+\frac{2m}{g}\right)\times\frac{3[1+(4m/g)y^{1/4}]^2+[31+(4m/g)y^{1/4}]y}{3[1+(4m/g)y^{1/4}]^2+[13+(4m/g)y^{1/4}]y}. \quad (4.26)$$

For the massless Schwinger model Eq. (4.26) reduces to

$$\frac{m_+}{g}=\left(\frac{3+31y}{3+13y}\right)\frac{1}{2y^{1/4}}, \quad (4.27)$$

which is plotted in Fig. 15. Note that m_+ is considerably larger than m_-. We suspect that if the equations for m_- and m_+ could be obtained in higher orders, the trend $m_+\to 2m_-$ would emerge and this state would disappear into the continuum. This would reflect the fact that the continuum Schwinger model describes a free neutral boson with $m_-=g/\sqrt{\pi}$. Perhaps finding $m_+\approx 0.8(2m_-)$ in a fourth-order lattice expansion is rather good.

Now consider Eqs. (4.20) and (4.26) for $m\neq 0$. Consider the quantity $1-m_+/2m_-$ for various

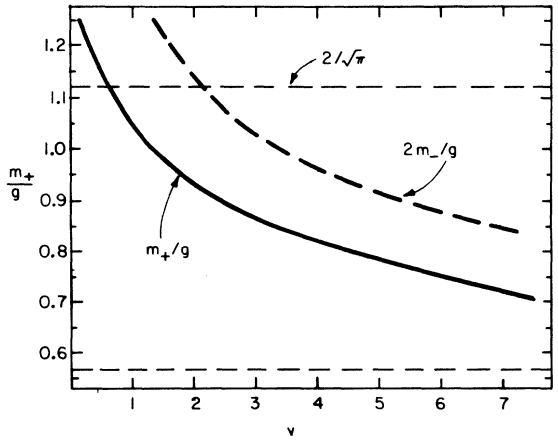

FIG. 15. A plot of Eq. (4.24).

values of m. A simple analysis of the continuum massive Schwinger model suggests that the $|1+\rangle$ state is a stable particle for any m different from zero. Before we argue this point, consider Fig. 16, which shows $(1-m_+/2m_-)$ as a function of m for $y=2.25$. Clearly the tendency for the $|1+\rangle$ state to become better bound by the $m\bar{\psi}\psi$ term in H is apparent in lattice perturbation theory. We expect that the ordinate of Fig. 16 will decrease to zero once higher orders are calculated.

To support our assertions concerning the continuum massive Schwinger model recall that it can be written in terms of an equivalent interacting boson field ϕ.[6] The Hamiltonian reads

$$H=\tfrac{1}{2}\int\left[\dot{\phi}^2+\left(\frac{\partial\phi}{\partial x}\right)^2+\frac{g^2}{\pi}\phi^2-2K\cos(2\sqrt{\pi}\,\phi)\right]dx, \tag{4.28}$$

where[12]

$$K=m\frac{g}{2\pi\sqrt{\pi}}e^{\gamma},\quad \gamma=\text{Euler's constant}=0.577\ldots. \tag{4.29}$$

Suppose m is small and $g/\sqrt{\pi}\gg m$ so the bosons can be treated as nonrelativistic and weakly interacting. Then the ϕ^4 interaction in Eq. (4.28) should be the most important nonlinearity. Its coefficient is negative, so it gives an attractive δ-function potential in the nonrelativistic domain. Such a potential always binds a state with the same quantum numbers as $|1+\rangle$ $(PC=++)$ in one spatial dimension. Thus we strongly suspect that the massive Schwinger model has a bound state for arbitrarily small m which tends to the continuum as $m\to 0$.

Next let us calculate $\partial(E_1-E_0)/\partial\mu$ at $m=0$ by lattice methods for the state $|1-\rangle$ and compare with the known result in the massive Schwinger model.[6] We see from Eq. (4.16) that

$$E_1-E_0=1+2y-10y^2+\mu(2-4y+56y^2)+O(\mu^2). \tag{4.30}$$

Therefore,

$$\left.\frac{\partial(E_1-E_0)}{\partial\mu}\right|_{m=0}=\left.\frac{\partial m_-}{\partial m}\right|_{m=0}=2(1-2y+28y^2), \tag{4.31}$$

which also may be written as a diagonal Padé approximant and extrapolated to large y. We compute

$$\left.\frac{\partial m_-}{\partial m}\right|_{m=0}=2\left(\frac{1+12y}{1+14y}\right)\xrightarrow[y\to\infty]{}1.71. \tag{4.32}$$

To compare with the continuum theory, note from Eq. (4.28) that taking $m\neq 0$ causes the replacement in the coefficient of ϕ^2

$$m_-^2=g^2/\pi\to g^2/\pi+(2g/\sqrt{\pi})me^{\gamma}\cong(g/\sqrt{\pi}+me^{\gamma})^2. \tag{4.33}$$

Therefore,

$$\left.\frac{\partial m_-}{\partial m}\right|_{m=0}=e^{\gamma}=1.78. \tag{4.34}$$

The detailed agreement between Eqs. (4.34) and (4.32) is a pleasant surprise.

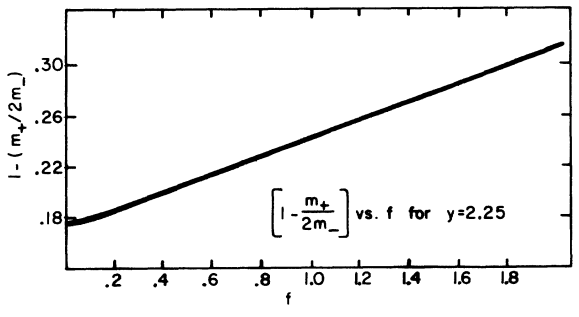

FIG. 16. A plot of the fractional distance the scalar state lies below the two-boson continuum. The horizontal axis is labeled with $f\equiv 4m/g$, a dimensionless measure of the fermion mass.

V. DISCUSSION

We hope that this article has demonstrated that high-order strong-coupling calculations can be carried out conveniently in simple gauge theories on a spatial lattice. When these series expansions are improved via Padé approximants, the results can be extrapolated far from the strong-coupling domain and good agreement with continuum theories results. We hope that this agreement will transcend the particulars of the model we chose to study here.

It was also encouraging that the actual strong-coupling calculations were very systematic and simple. With the aid of computers the calculations sketched here can certainly be extended several more orders. Work in this direction has begun. It is also clear that these calculations are very similar to spin-lattice high-temperature expansions used so profitably in statistic mechanics. We anticipate considerable help in our project from our solid-state friends.

The reader, no doubt, has many reservations about our great expectations. For example, we defined the mass of the composite particle as the gap in its energy-momentum relations, $E(p)$, at

zero momentum. Since the lattice does not have full translation invariance, this definition may not agree with a calculation of

$$\left(\frac{1}{p}\,\frac{dE}{dp}\bigg|_{p=0}\right)^{-1}.$$

In addition, one would like to know how the curve in Fig. 14 varies as we calculate to higher order. We do not have thorough answers for these questions at this time, but they are under study.

Note added in proof. The calculations discussed here have been extended to $O(y^4)$. Our methods prove to be particularly good for dimensionless quantities such as mass ratios and various low-energy matrix elements. Some calculations for $(3+1)$-dimensional gauge theories are completed and results will be presented shortly.

ACKNOWLEDGMENT

Two of the authors (J. K. and L. S.) thank A. Neveu and J. Gervais for their hospitality at Ecole Normale Superieure during the Conference on Extended Hadrons in Field Theory, where this work was completed. J. K. thanks D. K. Sinclair for checking much of the analysis presented here.

---

*Work supported in part by NSF under Grant No. GP-38863.

†Work supported in part by the National Science Foundation.

[1]K. G. Wilson, Phys. Rev. D 10, 2445 (1974).

[2]John Kogut and Leonard Susskind, Phys. Rev. D 11, 395 (1975).

[3]Leonard Susskind, lectures given at the Bonn Summer School, 1974 (unpublished).

[4]John Kogut and Leonard Susskind, invited talks at the Conference on Extended Systems in Field Theory, Ecole Normale Superieure, 1975 (unpublished).

[5]J. Schwinger, Phys. Rev. 128, 2425 (1962); J. Lowenstein and J. Swieca, Ann. Phys. (N. Y.) 68, 172 (1971); A. Casher, J. Kogut, and Leonard Susskind, Phys. Rev. Lett. 31, 792 (1973).

[6]J. Kogut and Leonard Susskind, Phys. Rev. D 11, 3594 (1975); S. Coleman, R. Jackiw, and Leonard Susskind, Harvard report, 1975 (unpublished).

[7]P. Jordan and E. P. Wigner, Z. Phys. 47, 631 (1928), reprinted in J. Schwinger, *Quantum Electrodynamics* (Dover, New York, 1958), p. 41.

[8]For a review and references to the literature see J. Kogut and Leonard Susskind, Phys. Rep. 8C, 75 (1973).

[9]J. Schwinger, Phys. Rev. Lett. 3, 296 (1959).

[10]A. Messiah, *Quantum Mechanics* (North-Holland, Amsterdam, 1962), Vol. II.

[11]Some introductory remarks on Padé approximants can be found in H. Eugene Stanley, *Introduction to Phase Transitions and Critical Phenomena* (Oxford Univ. Press, Oxford, 1971).

[12]The coefficient K is easily determined by requiring that products of bilinears $\bar{\psi}\psi$ yield identical Green's functions at short distances as $\cos(2\sqrt{\pi}\phi)$. Since the Schwinger model is superrenormalizable, such calculations are simple exercises in free-field theory. Our result has been checked against that of B. Klaiber, in *Lectures in Theoretical Physics*, edited by A. Barut and W. Brittin (Gordon and Breach, New York, 1968), Vol. X A.